

ROYAL AIRCRAFT ESTABLISHMENT

Technical Report 72071

Received for printing 20 March 1972

AIR DENSITY AT HEIGHTS NEAR 200 km FROM ANALYSIS OF THE ORBIT OF 1969-20B

by

Doreen M. C. Walker

SUMMARY

The rocket of Cosmos 268, 1969-20B, entered orbit on 5 March 1969, with an initial perigee height of 230 km and inclination of  $48.40^{\circ}$ . Accurate orbits were computed at RAE from all available observations. Using the values of perigee height from the RAE orbit and decay rates from Spacetrack bulletins, 103 values of density have been calculated between July 1969 and February 1970. On three occasions when geomagnetic activity was strong there were sudden increases in density. When the density was corrected to a fixed height, the semi-annual variation was apparent. There was a strong minimum in July 1969, a maximum in October-November 1969 and a weak minimum in January 1970.

AD 749008



CONTENTS

	<u>Page</u>
1 INTRODUCTION	3
2 ORBITAL DECAY RATE	3
3 PERIGEE HEIGHT	4
3.1 The 'perigee height parameter' $Q$	4
3.2 Calculation of perigee height $y_p$	5
4 CALCULATION OF AIR DENSITY	5
5 RESULTS	6
5.1 Variation of density with time	6
5.2 The day-to-night variation	7
5.3 Comparison with geomagnetic and solar indices	7
5.4 The semi-annual variation	8
5.5 Variation with height	8
6 DISCUSSION OF RESULTS	9
7 CONCLUSIONS	10
References	11
Illustrations	Figures 1-11
Detachable abstract cards	-



## 1 INTRODUCTION

The air density at heights near 180 km has been determined from the orbit of 1967-31A<sup>1</sup>, between July 1968 and September 1969, and at heights near 150 km, between December 1969 and August 1970, from 1969-108A<sup>2</sup>. These two studies leave a gap in time between September and December 1969 and the present study was undertaken to evaluate the variations in density between the two, and to overlap at each end. Unfortunately there was no satellite available with a perigee height below 200 km. The satellite selected was the rocket of Cosmos 268, 1969-20B. The density was evaluated over the last seven months of the satellite's life, from July 1969 to February 1970. During this time the perigee height decreased from 218 km to 155 km.

Cosmos 268, 1969-20A, was launched on 5 March 1969, and its rocket, 1969-20B, entered an orbit with an initial perigee height of 230 km, an apogee height of 2170 km, and inclination  $48.40^\circ$ . This rocket, about 8 m long and 1.65 m in diameter<sup>3</sup>, was a good object for optical observation from Britain, and because of its interest for upper-atmosphere research, it was given high priority for observing by the British optical and radar tracking stations, including the Hewitt camera at Malvern. Accurate orbits have been computed at RAE from all available observations<sup>4</sup>, the perigee heights having an average sd of about 200 m. In the present paper these perigee heights were used, together with the orbital decay rates calculated from USAF Spacetrack elements: 103 values of air density at heights between 185 km and 253 km were obtained at dates between 17 July 1969 and 8 February 1970.

## 2 ORBITAL DECAY RATE

The orbital decay rate was found with adequate accuracy from the USAF Spacetrack 5-card elements, of which 114 sets were issued during the seven months. As in previous studies<sup>1,2</sup> the values of the mean anomalistic motion  $n$  (rev/day) were tabulated and differenced to give values of  $\Delta n$ , each of which was divided by the corresponding time interval  $\Delta t$  (day) to give values of  $\dot{n} \approx \Delta n / \Delta t$  (rev/day<sup>2</sup>). Any erroneous value of  $n$  causes an up-down pattern in  $\dot{n}$ , i.e. one value is too high and the next too low, or *vice versa*. After inspecting the values of  $\dot{n}$  up to MJD 40608, six values of  $n$  were eliminated which led either to up-down patterns or to time intervals  $\Delta t$  less than 24 hours; one more value of  $n$  was omitted over the final phase, MJD 40608-MJD 40628, because of an up-down tendency, but the minimum limit on  $\Delta t$  was reduced to 6 hours.



The remaining 106 values of  $\dot{n}$  are plotted as circles in Fig.1, and the values from the RAE orbits are plotted as triangles. The RAE values are for specific dates while the  $\dot{n}$  values from Spacetrack are averages over a time interval  $\Delta t$ . With this difference taken into account, the two sets show excellent agreement.

### 3 PERIGEE HEIGHT

#### 3.1 The 'perigee height parameter' Q

The perigee distance  $a(1 - e)$ , where  $a$  is the semi major axis and  $e$  the eccentricity, suffers a regular oscillation caused by the effect of the odd zonal harmonics in the Earth's gravitational potential. For 1969-20B at an inclination  $i$  of  $48.4^\circ$  this perturbation<sup>5</sup> amounts to  $5.10 \sin \omega$  km, where  $\omega$  is the argument of perigee. In the Spacetrack orbital elements this perturbation is taken to be  $6.8 \sin i \sin \omega = 5.09 \sin \omega$  km, and is subtracted from the values of  $e$ . Since the Spacetrack perigee distances are not likely to have an accuracy better than 0.5 km, the difference of 0.01 km is not significant.

It is useful to define a 'perigee height parameter',  $Q$  say, which is free of the effects of the odd zonal harmonics. The obvious definition to use is

$$\left. \begin{aligned} Q &= [a(1 - e) - R]_{\text{Spacetrack}} \\ \text{or} \quad Q &= [a(1 - e) - R]_{\text{RAE}} + 5.10 \sin \omega \end{aligned} \right\} \quad (1)$$

where  $R$  is the Earth's equatorial radius (6378.16 km). The quantities given by these equations should be identical, apart from observational errors, and  $Q$  should decrease slowly under the combined influence of air drag and luni-solar perturbations.

Fig.2 gives values of  $Q$  from the Spacetrack elements (circles) and the RAE orbits (triangles). The RAE values all have standard deviations less than 350 m, and should be more accurate than the Spacetrack values. A smooth curve has been drawn through the values of  $Q$  in Fig.2, giving more weight to the accurate RAE values, but the real variation of  $Q$  with time will not be smooth because of the variations in  $\dot{n}$  apparent in Fig.1.



### 3.2 Calculation of perigee height $y_p$

The actual perigee height  $y_p$  above the Earth is found from  $Q$  by restoring the odd-zonal-harmonic oscillation ( $5.10 \sin \omega$ ), subtracting the local Earth radius at latitude  $\phi_p$ , which differs from  $R$  by  $21.38 \sin^2 \phi_p = 11.95 \sin^2 \omega$  km, and adding the small amount by which the actual perigee distance<sup>6</sup> differs from  $a(1 - e)$ , namely  $0.83 - 1.74 \sin^2 \omega$  km. Thus we find

$$\left. \begin{aligned} y_p &= Q + 0.83 + 10.21 \sin^2 \omega - 5.10 \sin \omega \\ &= Q + q \end{aligned} \right\} \quad (2)$$

The variation of  $q$  with  $\omega$  is given in Fig.3, which shows that the combined effect of Earth oblateness and odd harmonics can alter perigee height by up to 16 km; as usual the maximum perigee height occurs at  $\omega = 270^\circ$ .

Fig.4 shows the values of  $y_p$  for 1969-20B as given by equation (2), with  $Q$  having the values given by the curve in Fig.2.

### 4 CALCULATION OF AIR DENSITY

The air density at a height  $H^*$  above perigee was found from the usual equation

$$\rho_A = \frac{0.157(1000\dot{n})}{10^6 \dot{n}^2 \delta} \left( \frac{e}{aH^*} \right)^{\frac{1}{2}} \frac{(1-e)^{1/2}}{(1+e)^{3/2}} \left\{ 1 - \frac{H^*}{8ae} \left( 1 - 8e + \frac{7H^*}{16ae} \right) + \frac{\varepsilon \sin^2 i \cos 2\omega}{e} \right\} \quad \dots (3)$$

where  $H^*$  is the estimated value of  $H$  at perigee height, and may be in error by up to 25% without incurring an error of more than 1.2% in  $\rho_A$ . The assumed variation of  $H$  with height is given in Fig.5, the values having been taken from the latest available model atmosphere of Jacchia<sup>7</sup>. Equation (3) is valid if  $3H^*/a < e < 0.2$ , conditions that are satisfied for all but the last three values of  $\dot{n}$ . The values of  $\rho_A$  in equation (3) are obtained in  $\text{kg/m}^3$  if  $H^*$  and  $a$  are in km, the area/mass parameter  $\delta$  is in  $\text{m}^2/\text{kg}$ ,  $\dot{n}$  is in rev/day and  $\dot{n}$  in  $\text{rev/day}^2$ .

The value of the area/mass parameter  $\delta$  is not known accurately for Cosmos 316, and a constant value,  $0.0246 \text{ m}^2/\text{kg}$ , was used, corresponding to a mass/area ratio of  $83 \text{ kg/m}^2$ . This value was chosen so that the values of density at the average of the semi-annual variation at heights between 180 and 190 km were in agreement with Jacchia's model<sup>7</sup> for the appropriate value of exospheric temperature, 1100 K.



Equation (3) gives values of  $\rho_A$ , the air density at a height  $y_A = y_p + \frac{1}{2}H^*$ . In examining day-to-day variations in density we need to convert the values of density to a fixed height,  $y_B$ , say, which may most appropriately be taken as the mean value of  $y_A$  over a suitable time interval. The density  $\rho_B$  at height  $y_B$  is calculated from the equation

$$\rho_B = \rho_A \exp \left( \frac{y_A - y_B}{H_B} \right) \quad (4)$$

where  $H_B$  is the value of  $H$  at height  $y_B$ . If  $H_B$  is in error by  $N\%$ , the use of equation (4) will lead to an error of approximately  $[(y_A - y_B)N/H_B]\%$  in  $\rho_B$ . Since  $H_B$  may be in error by up to perhaps 10% as a result of day-to-day variations in  $H$ , the value of  $(y_A - y_B)/H_B$  needs to be kept as small as possible. It was therefore necessary to split the total time interval into several parts. The breaks were made at MJD 40540, 40616 and 40624, and the values of the various parameters during the three time intervals are given in Table 1.

Table 1

The four sets of values of  $y_p$ ,  $H^*$ ,  $y_B$  and  $H_B$

Time interval MJD	Mean $y_p$ km	$H^*$ km	$y_B$ km	$H_B$ km
40419-40540	225	40	245	43
40540-40616	203	34	220	38.5
40616-40624	185	30	200	33.5
40624-40626	172	26	185	29.5

## 5 RESULTS

### 5.1 Variation of density with time

The values of  $\rho_B$  obtained are plotted as points joined by lines in Fig. 6. From MJD 40419 to MJD 40540 the values of  $\rho_B$  are for a height of 245 km, i.e. they are values of  $\rho_{245}$ ; from MJD 40540 to MJD 40616 the density is for a height 220 km, but the quantity plotted is  $0.538\rho_{220}$ , the numerical factor 0.538 being introduced to avoid discontinuity; from MJD 40616 to 40624 and from MJD 40624 to 40626, the values plotted are  $0.305\rho_{200}$  and  $0.187\rho_{185}$  respectively, the numerical factor being included for the same reason.



The quantity plotted at the top of Fig.6 is the sun-perigee angle, with the local time at perigee marked on the curve.

### 5.2 The day-to-night variation

In Fig.6 the semi-annual variation in air density is somewhat obscured by the day-to-night variation, and a correction for day-to-night variation must therefore be made.

This correction was calculated by using Ref.7. From Table 6 of Ref.7, values of  $\rho/\bar{\rho}$  are plotted against  $T/T_0$  for various heights in Fig.7, where  $\rho$  is the value of density for a given temperature  $T$ ,  $\bar{\rho}$  is the density at temperature 1000 K and  $T_0$  is the minimum night-time temperature, taken as 870 K. The value of  $T/T_0$  appropriate to the local time, solar declination and perigee latitude at each of the 103 calculated values of density, was then obtained from Table 1 of Ref.7; and hence, knowing the perigee heights from Fig.4, values of  $\rho/\bar{\rho}$  were found from Fig.7. These are plotted against MJD in Fig.8. The correction for the day-to-night variation can then be made by dividing each calculated value of density by the appropriate value of  $\rho/\bar{\rho}$ . The corrected values of density are plotted in Fig.9, numerical factors again being included to avoid discontinuity. The quantities plotted at the top of Fig.9 are the solar radiation energy on a wavelength of 10.7 cm,  $S_{10.7}$ , as measured by NRC, Ottawa and the daily geomagnetic index  $A_p$  as given by the Institut für Geophysik, Göttingen, plotted with a 12-hour time lag.

### 5.3 Comparison with geomagnetic and solar indices

Between July 1969 and February 1970 there were three occasions when geomagnetic disturbances were strong enough to give values of  $A_p$  greater than 40. These three disturbances, at MJD 40430, 40495 and 40535, are accompanied by marked increases in air density, as Fig.9 shows.

Previous studies<sup>1,2</sup> have suggested that at heights below 200 km there is little resemblance between the variations in air density and in the solar 10.7-cm radiation, which is a rough measure of the extreme ultraviolet radiation. The height of 1969-20B is slightly over 200 km until the last 15 days of the satellite's life, but the correlation between the density values and  $S_{10.7}$  is not very strong. However there are some occasions when maxima and particularly minima of the solar activity coincide with maxima or minima in density. For example the minima in density, from Fig.9, at MJD 40422, 40450, 40478, 40510, 40565, 40595 and 40622 all occur when the values of  $S_{10.7}$  are



at minima. There are also three increases in density which correspond with rises in solar activity, namely at MJD 40460, 40515 and 40600. Of these three the largest is that around MJD 40510, amounting to about 40% between MJD 40596 and MJD 40603.

#### 5.4 The semi-annual variation

If the peaks of density at the times of geomagnetic disturbance are ignored, the overall pattern of the remaining values is that associated with the semi-annual variation. The two minima are in late July 1969 and early January 1970, and there is a maximum between these two dates, at October-November 1969. The values of density at semi-annual maximum and minima are given in Table 2. The values recorded are those sustained over 10 days (excluding values at times of geomagnetic disturbance), and are marked as broken lines in Fig. 10.

Table 2  
Semi-annual maximum and minima in density  
in 1969-1970 at heights near 240 km

	Central date	Values of $\rho_{245} \text{ } \mu\text{g/m}^3$
July minimum	1969 July 25	0.0520
October-November maximum	1969 October 31	0.0950
January minimum	1970 January 4	0.0808

The dates of the semi-annual maximum and minima are in agreement (within 10 days) with those obtained in the exosphere<sup>8</sup>, at heights near 1000 km, and at heights below 200 km<sup>1,2</sup>. The values in Table 2 have not been corrected for solar activity: there is no need for correction of the last two values, for which  $S_{10.7} = 145 \times 10^{-22} \text{ W m}^{-2} \text{ Hz}^{-1}$ , but the July minimum would be increased by about 18% if corrected to the same level of solar activity; with this correction the July value of  $0.0520 \text{ } \mu\text{g/m}^3$  would be increased to  $0.0614 \text{ } \mu\text{g/m}^3$ .

#### 5.5 Variation with height

The values of  $\rho_A$  are plotted against  $y_A$  in Fig. 10, to give the variation of density with height. The values plotted as circles are intended to represent average values of density derived from the orbit of 1969-20B, defined as those which give values of  $\rho_{245}$  between  $0.075 \text{ } \mu\text{g/m}^3$  and



0.100  $\mu\text{g}/\text{m}^3$  in Fig.9. Values outside this band are plotted as crosses. The dotted curve in Fig.10 represents the values given by Jacchia<sup>7</sup> for exospheric temperature 1100 K. This is the model to which the present values of density were scaled at heights between 180 and 190 km (see section 4). The broken curve in Fig.10 shows the Jacchia model for exospheric temperature 1000 K. Had the density values been scaled to this curve (at the same heights), they would be reduced by 8%. In the group of values at heights of 220-230 km an 8% decrease would result in more points lying above the broken curve than below it, whereas the opposite applies for the dotted curve: so it appears that the best model would be for exospheric temperature of about 1050 K. It can be concluded that the model fits the mean values well, and that the appropriate exospheric temperature, 1050 K, is close to the temperature that would be expected to fit the conditions ( $S_{10.7} \approx 145$ ).

## 6 DISCUSSION OF RESULTS

The density ratios obtained from this study for the semi-annual variation are 1.55 for the October 1969/July 1969 density ratio after the correction for solar activity; and 1.18 for the October 1969/January 1970 density ratio. These values fit in remarkably well with those obtained by Cook<sup>8</sup> from the orbit of 1964-63C at 1070 km, and are plotted in Fig.11, together with values<sup>1</sup> from 1967-31A at 185 km. Such good agreement in the trend of the variations suggests that the factors influencing the density in the exosphere also apply to the atmosphere around 200 km.

The sudden rise in density about MJD 40600 apparent in Fig.9 needs further examination, as this is a time when the density should still be fairly low following the January minimum. Also the increase in solar activity at the time of this large increase in density is not as great as in several of the peaks in previous months, where there was no such increase in density; so the increase in density is rather surprising. However the analysis of the orbits of 1965-16G and 1964-63C shows<sup>8</sup> that there was also a large increase in density at this time at heights near 1000 km. This would seem to confirm that the rise in density apparent in Fig.9 is real, and not due to a sudden change in cross-sectional area of the satellite. This finding illustrates once again that the 10.7-cm radiation is an imperfect index of the extreme ultraviolet radiation which influences the density, and therefore sometimes fails to show the correlation clearly. This increase in density at MJD 40600 was not detected in the analysis of 1969-108A<sup>2</sup> because this satellite had a lower perigee height and the density was evaluated at about 160 km, where the atmosphere is much less affected by solar activity.



## 7 CONCLUSIONS

(1) The main purpose of this paper is to establish the variations in air density at heights of 200-250 km, between July 1969 and February 1970. Fig.9 gives the results.

(2) It is noticeable that density increases sharply at times of geomagnetic disturbance, as expected, and that the 10.7-cm radiation energy is not always a good index of the influence of solar activity.

(3) The July 1969 semi-annual minimum is much stronger than that in January 1970, and this agrees remarkably well with results previously obtained<sup>8</sup> in the exosphere at heights near 1000 km (Fig.10).



REFERENCES

- | <u>No.</u> | <u>Author</u>                                  | <u>Title, etc.</u>  |
|------------|--|---|
| 1          | D.G. King-Hele<br>D.M.C. Walker                | Air density at heights near 180 km in 1968 and 1969, from the orbit of 1967-31A.<br><i>Planet. Space Sci.</i> , <u>19</u> , 297 (1971)<br>RAE Technical Report 70084 (1970)                                     |
| 2          | D.G. King-Hele<br>D.M.C. Walker                | Air density at heights near 150 km in 1970, from the orbit of Cosmos 316 (1969-108A).<br><i>Planet. Space Sci.</i> , <u>19</u> , 1637 (1971)<br>RAE Technical Report 71129 (1971)                               |
| 3          | J.A. Pilkington<br>D.G. King-Hele<br>H. Hiller | Table of Earth satellites. Volume 2, Parts 1 and 2: 1969 and 1970.<br>RAE Technical Report 71082 (1971)   |
| 4          | D.G. King-Hele<br>A.N. Winterbottom            | Analysis of the orbit of Cosmos 268 rocket (1969-20B).<br>RAE Technical Report 71202 (1971)   |
| 5          | D.G. King-Hele<br>G.E. Cook<br>D.W. Scott      | Evaluation of odd zonal harmonics in the geopotential, of degree less than 33, from analysis of 22 satellite orbits.<br><i>Planet. Space Sci.</i> , <u>17</u> , 629 (1969)<br>RAE Technical Report 68202 (1968) |
| 6          | Y. Kozai                                       | The motion of a close Earth satellite.<br><i>Astroncm. Journ.</i> , <u>64</u> , 367 (1959)  |
| 7          | L.G. Jacchia                                   | Revised static models of the thermosphere and exosphere with empirical temperature profiles.<br>Smithsonian Astrophys. Obs. Spec. Rpt. 332 (1971)   |
| 8          | G.E. Cook                                      | Density variations in the exosphere from June 1968 to December 1970.<br>RAE Technical Report 71150 (1971)   |



Fig.1

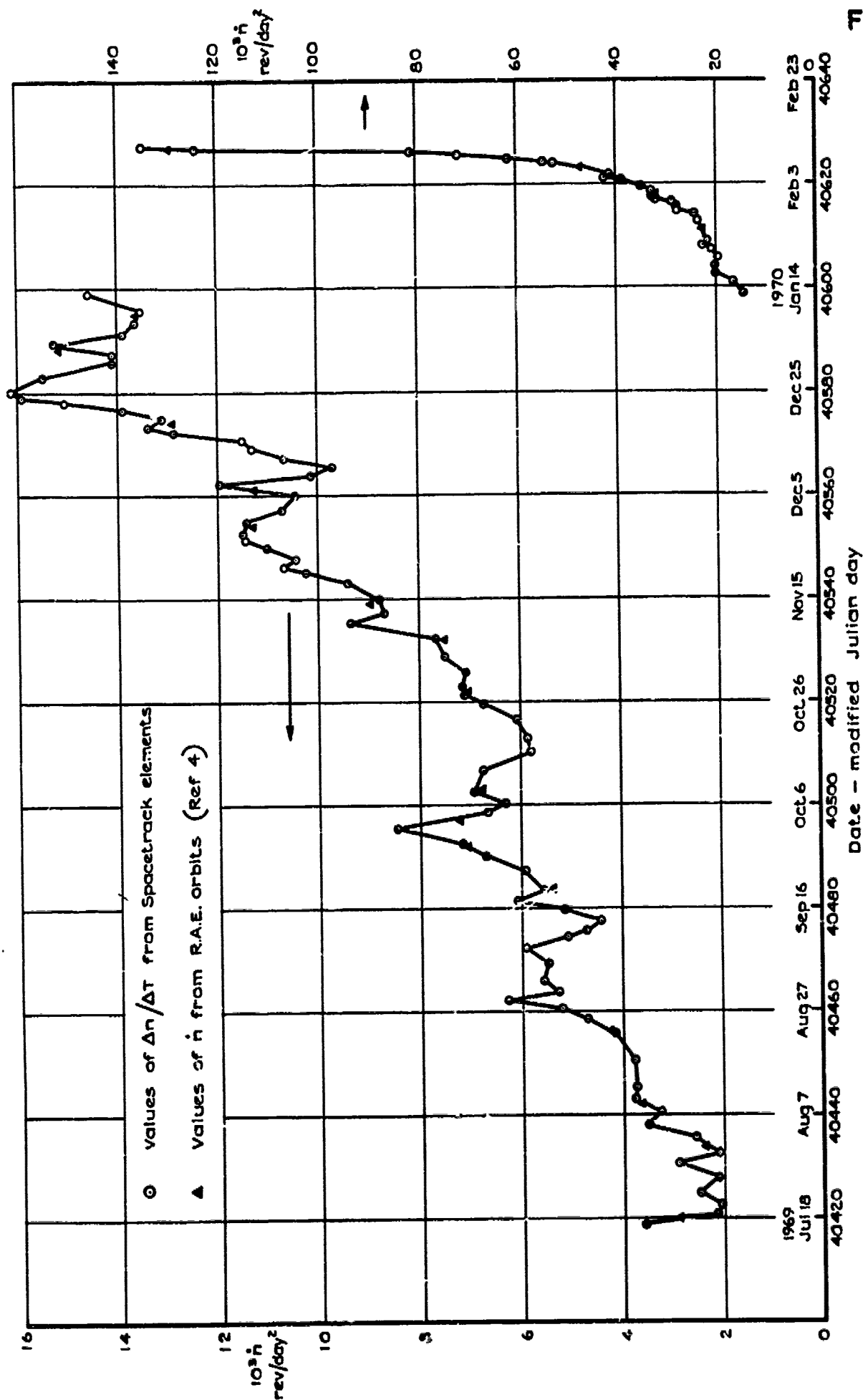
Fig.1 Values of orbital decay rate,  $\dot{h}$ , for 1969-20B



Fig.2

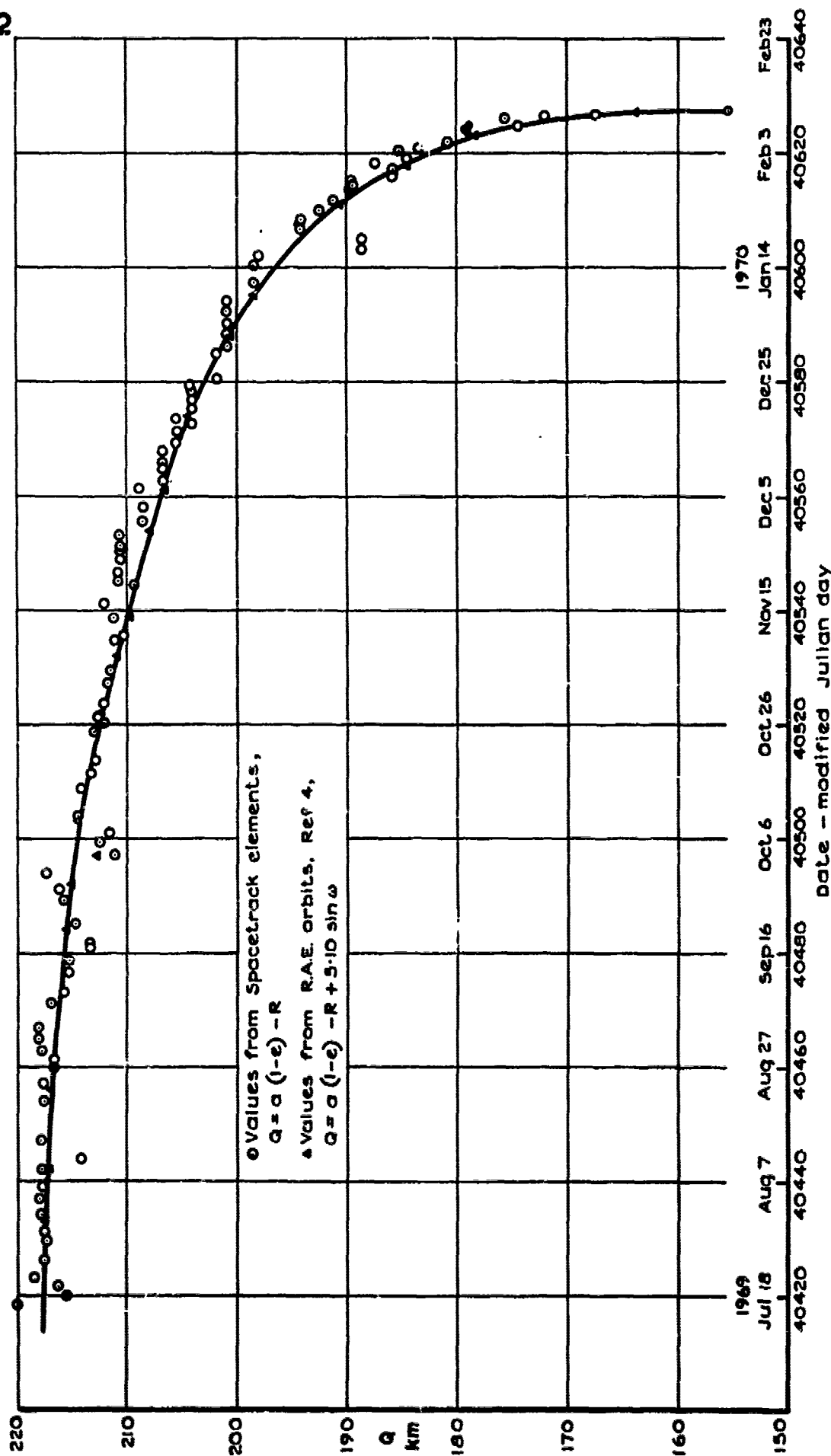


Fig.2 Values of the perigee height parameter Q, from R.A.E. and Spacetrack orbits



Fig.3

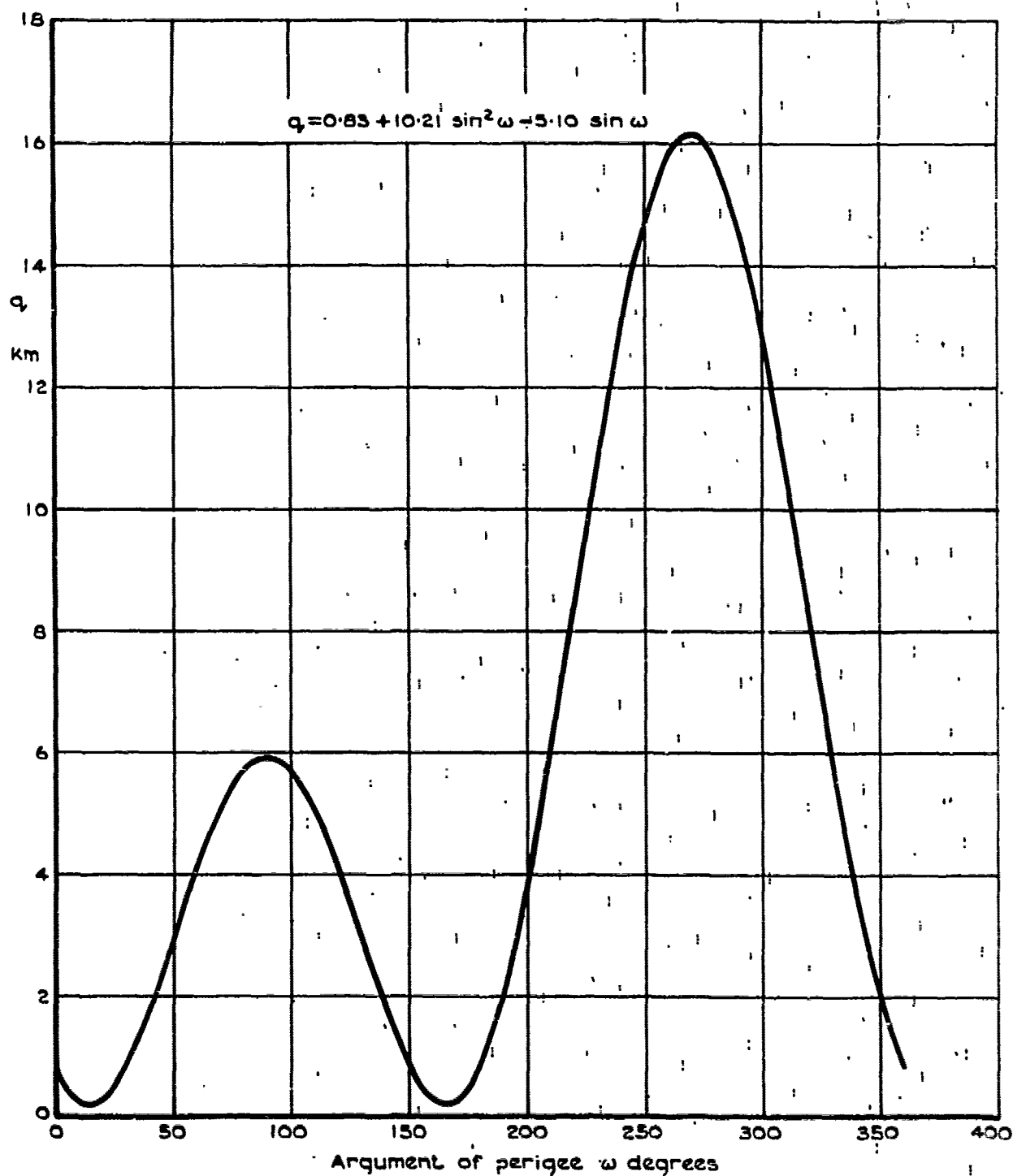


Fig.3 Variation of  $q$  with  $\omega$



Fig.4

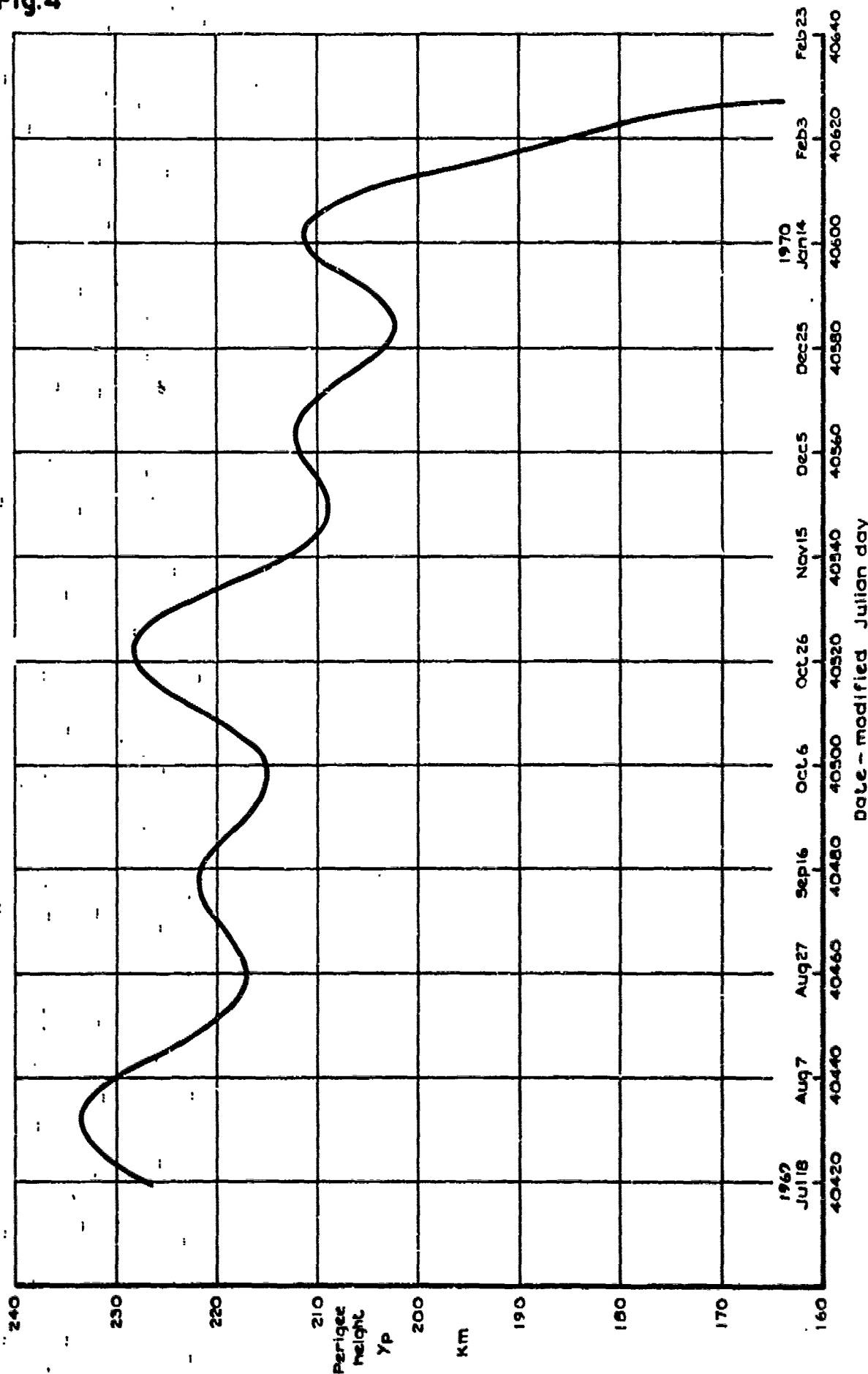


Fig.4 Variation of perigee height,  $y_p$

TR-72071



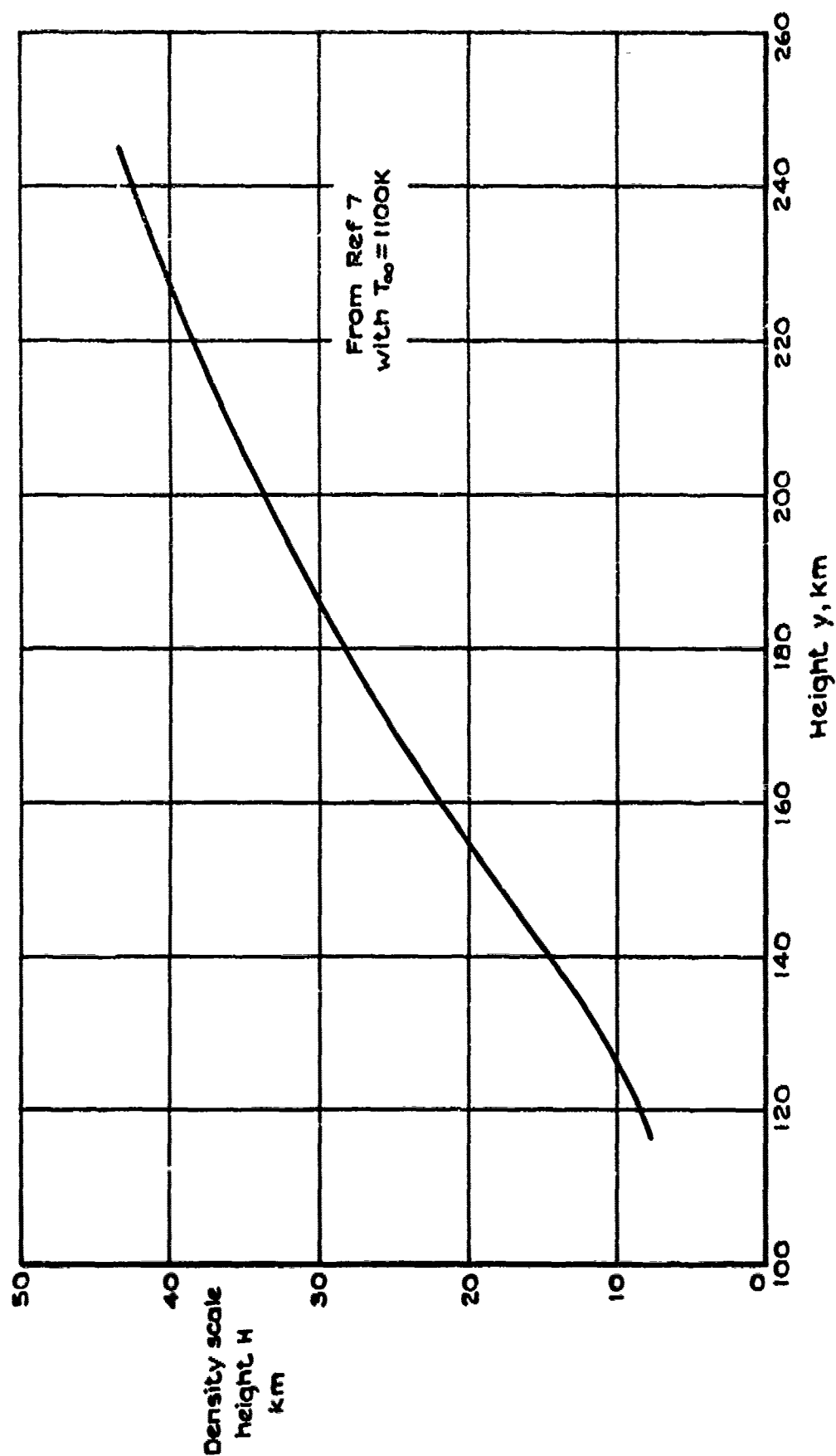


Fig. 5

Fig. 5 Variation of density scale height,  $H$  with height,  $y$



Fig.6

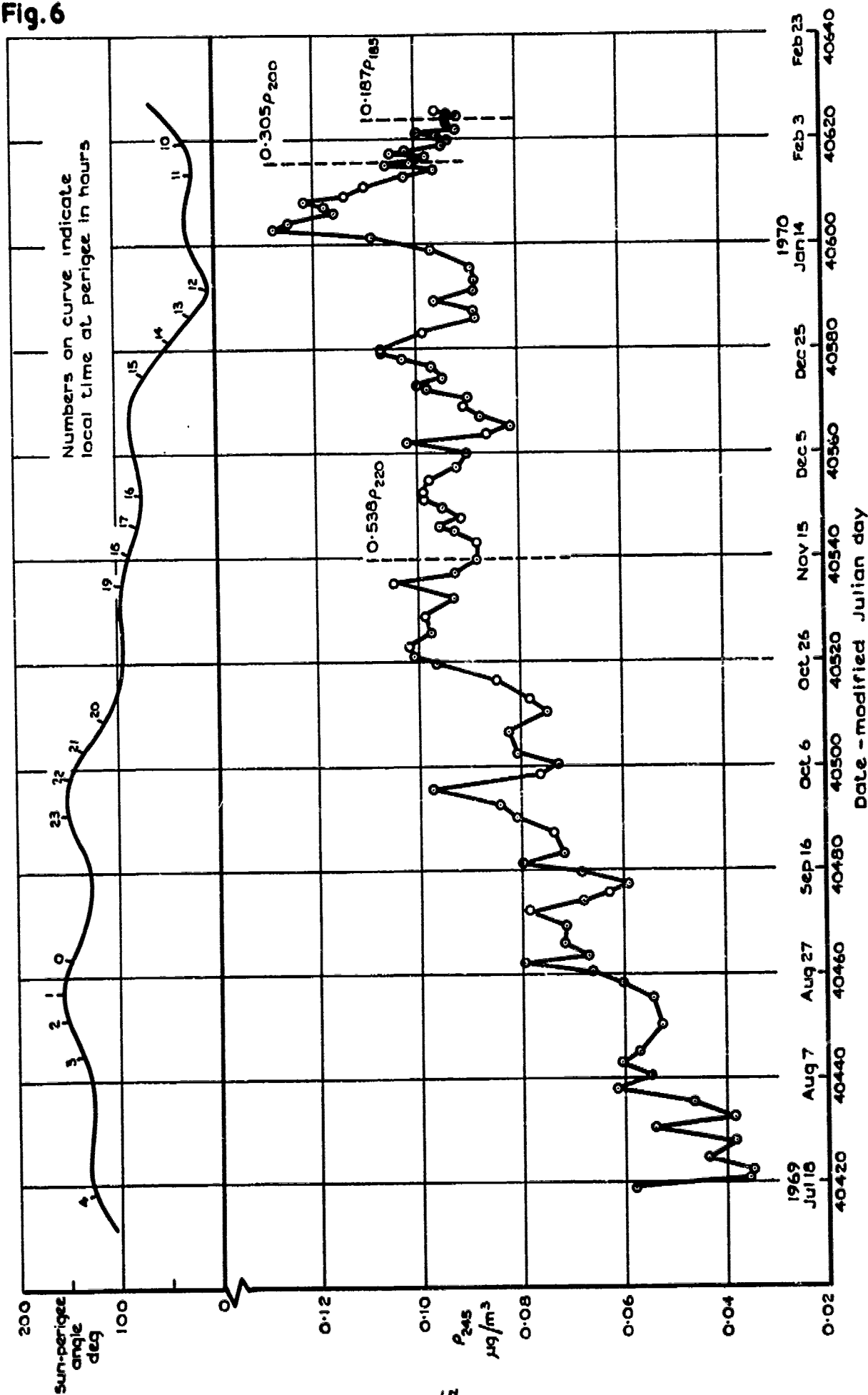


Fig.6 Values of density at standard heights, with values of Sun-perigee angle



Fig.7

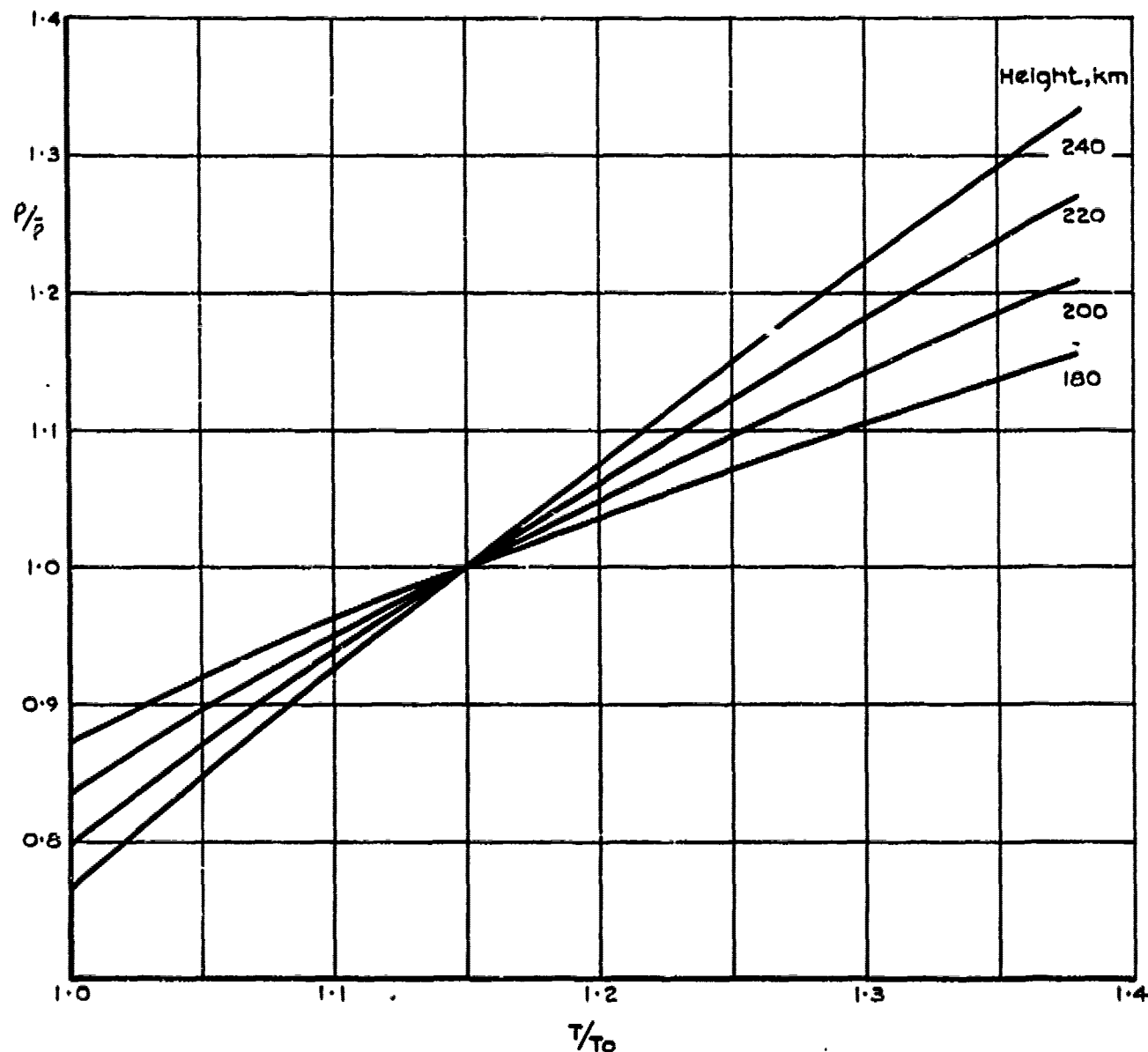


Fig.7 Variation of density  $\rho$  with temperature  $T$ , as given by Ref 7, with  $T_0 = 870$  K and  $\bar{\rho}$  the density at  $T = 1000$  K



Fig.8

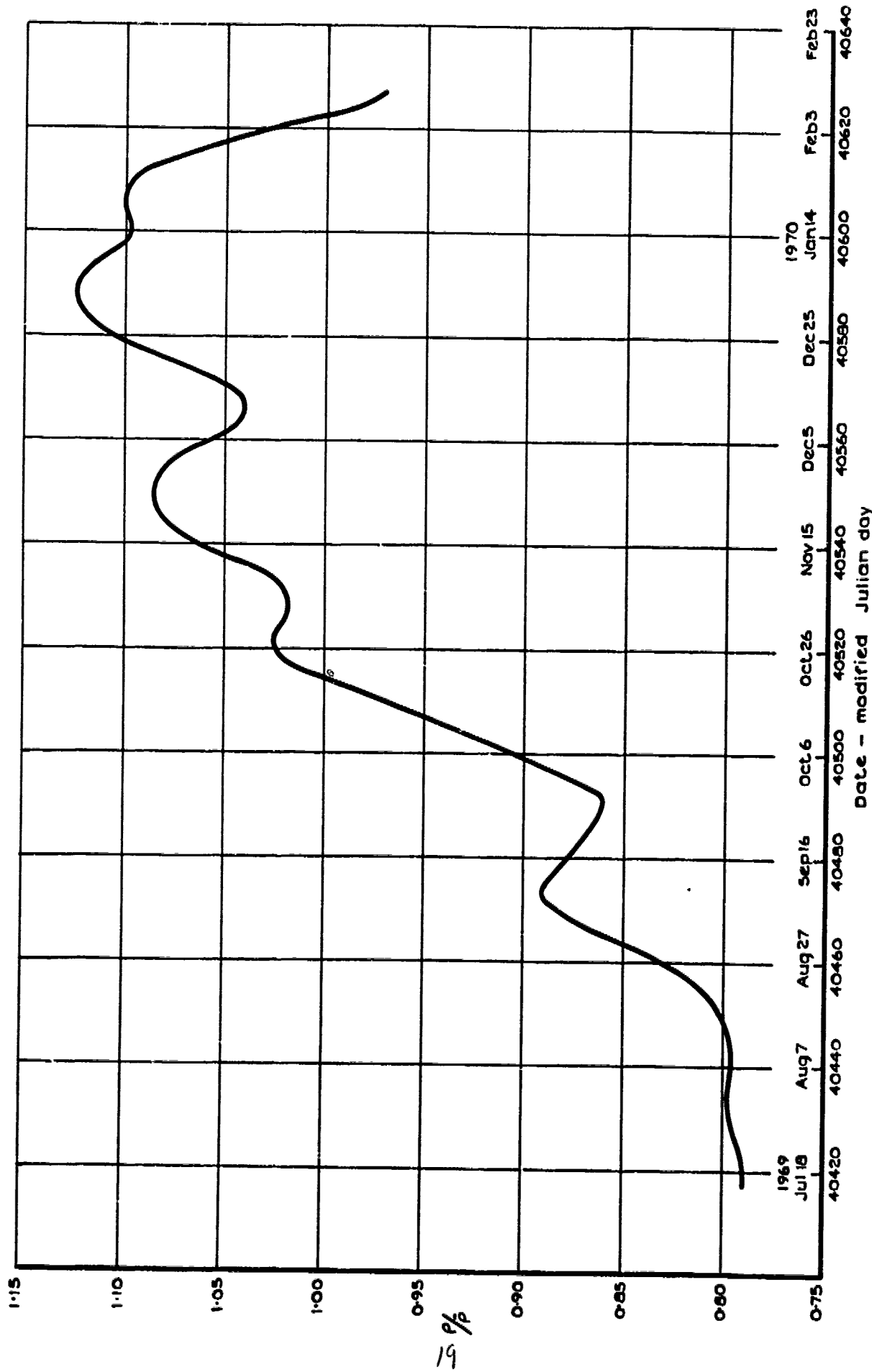


Fig.8 Variation in density due to changes in local time at perigee

T.R.72071



Fig. 9

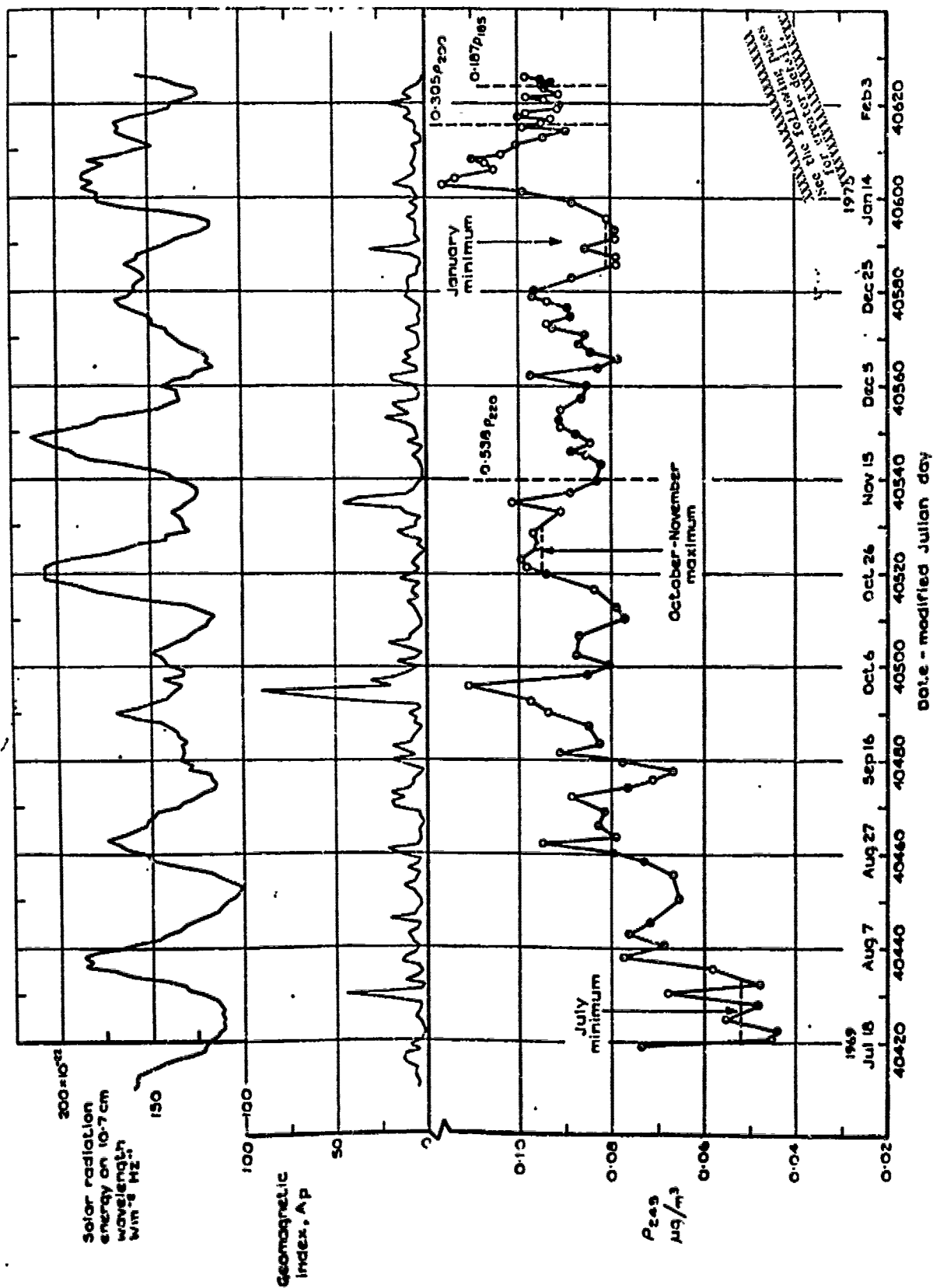


Fig. 9 Values of density at standard heights, corrected for day-to-night variation, with geomagnetic and solar indices



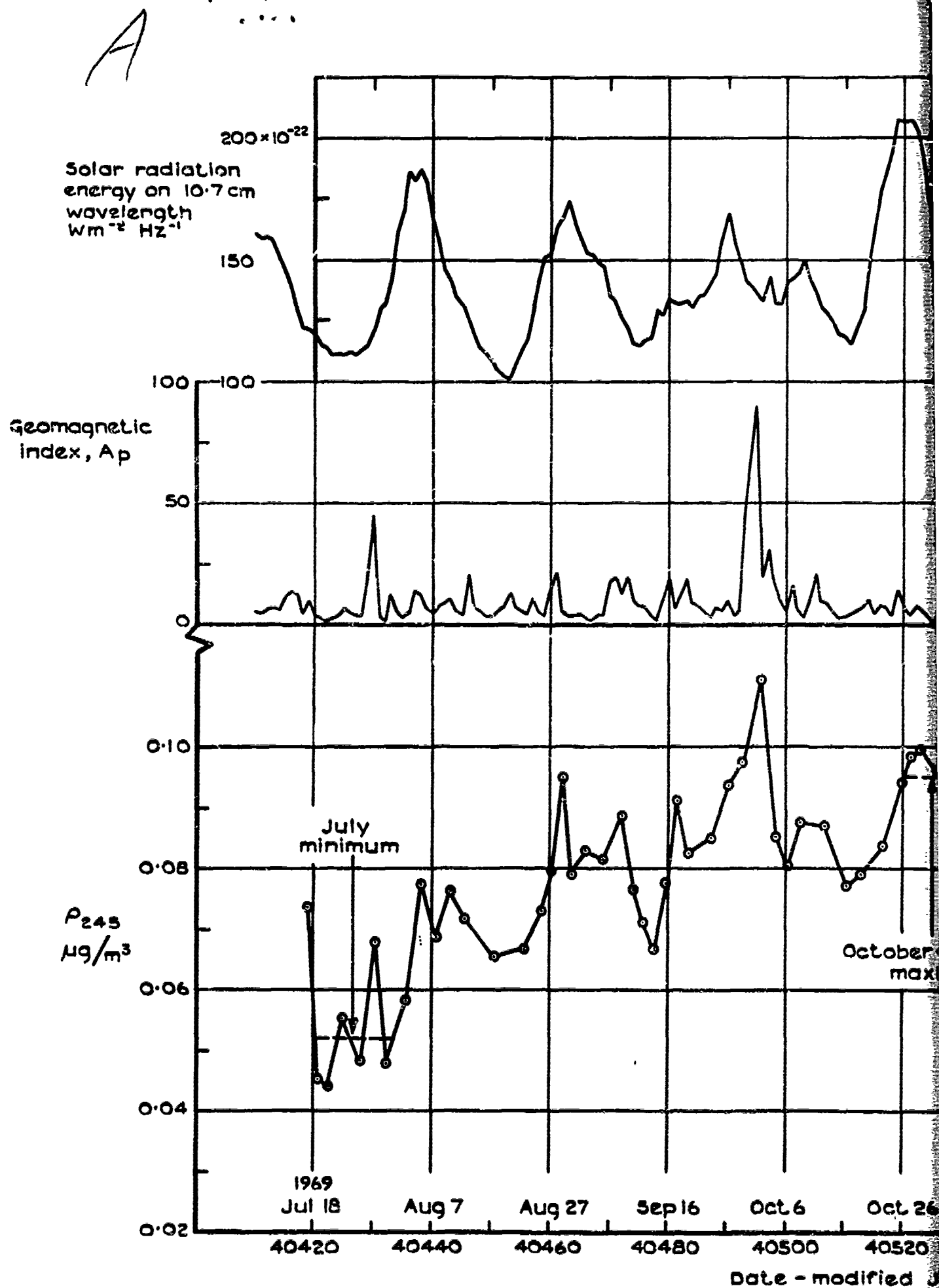


Fig. 9. Values of density at standard heights reported for the



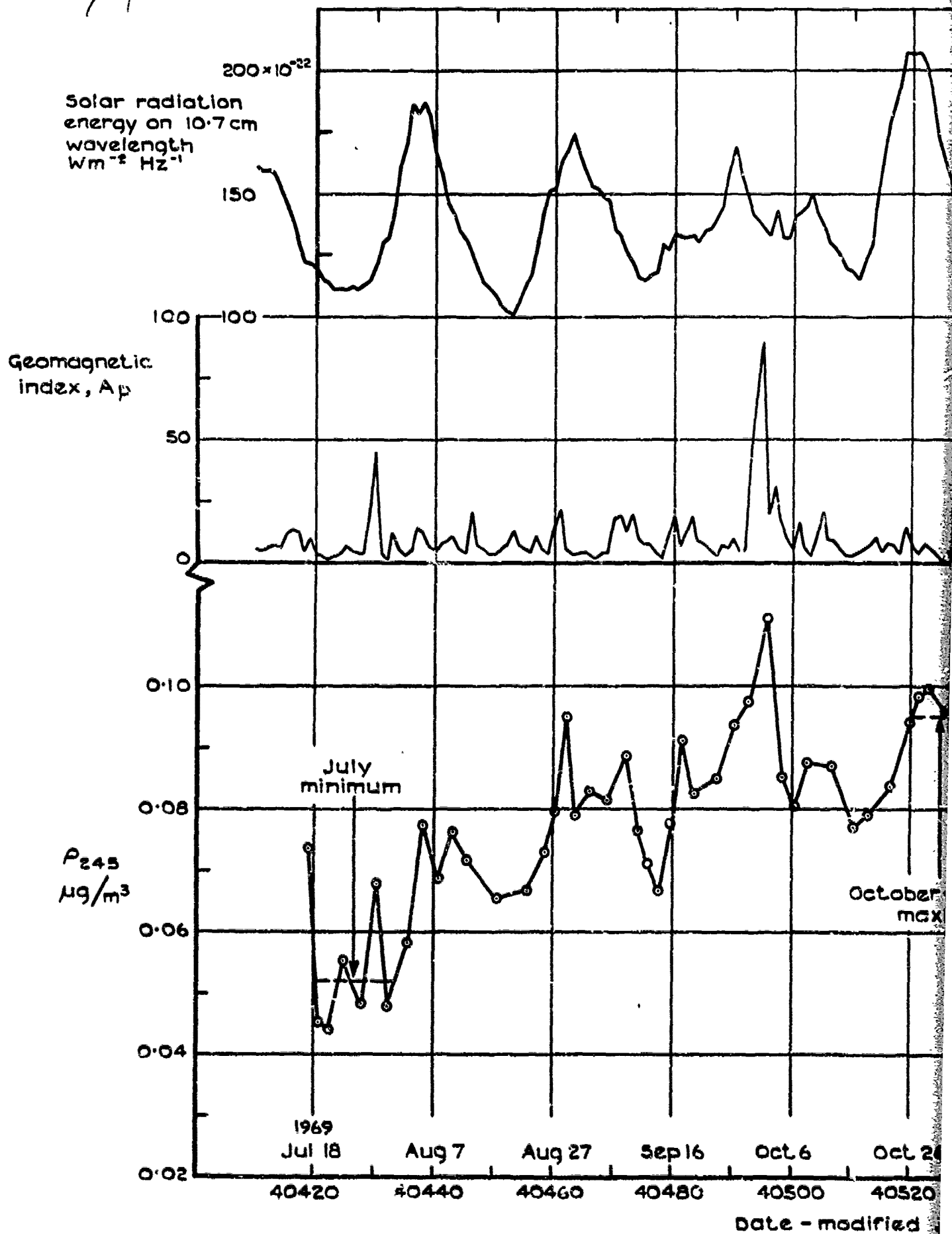


Fig. 9 Values of density at standard heights, corrected for day-to-night

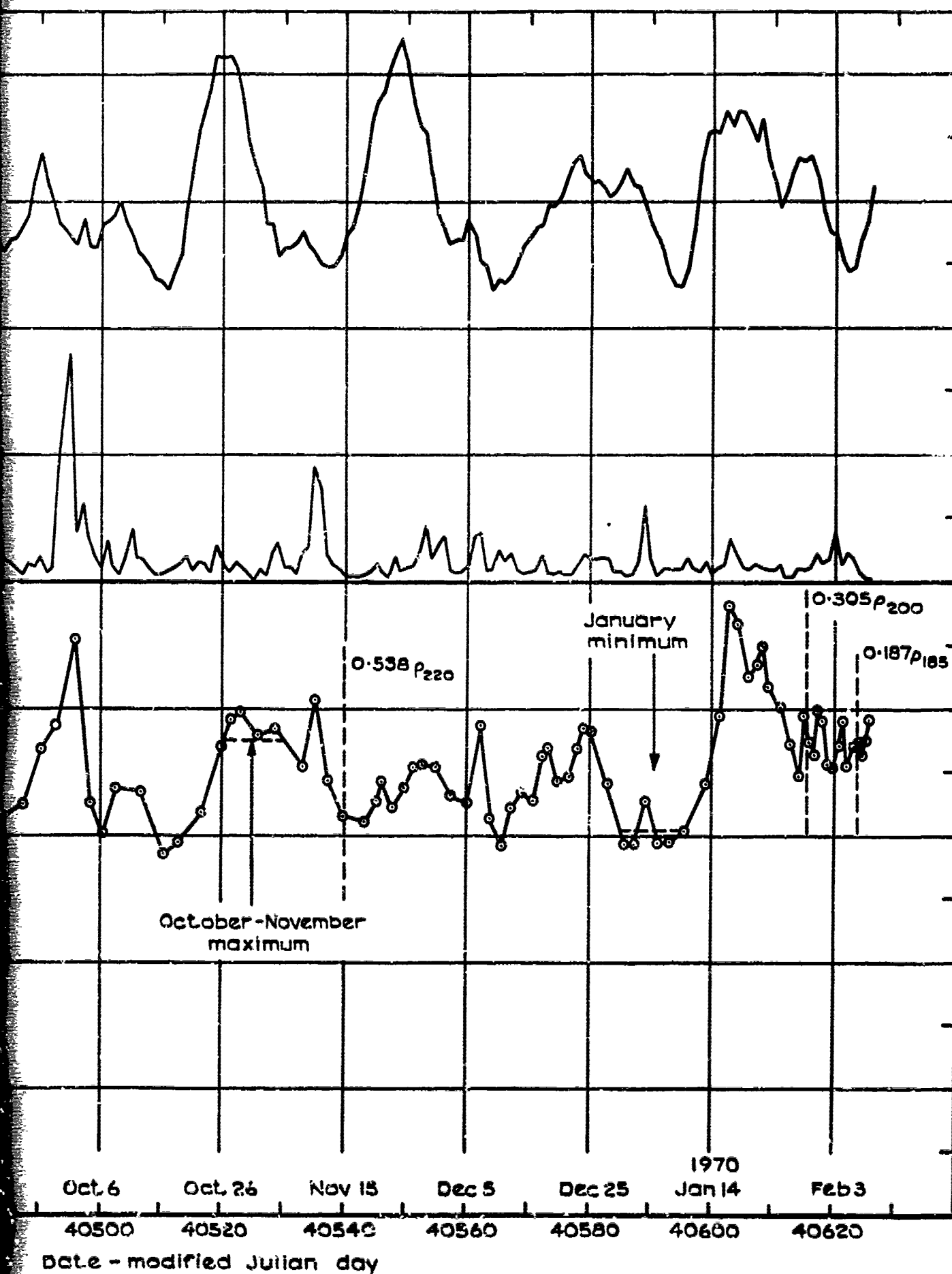
20.1

20.2



B

Fig. 9



ted for day-to-night variation, with geomagnetic and solar indices



Fig.10

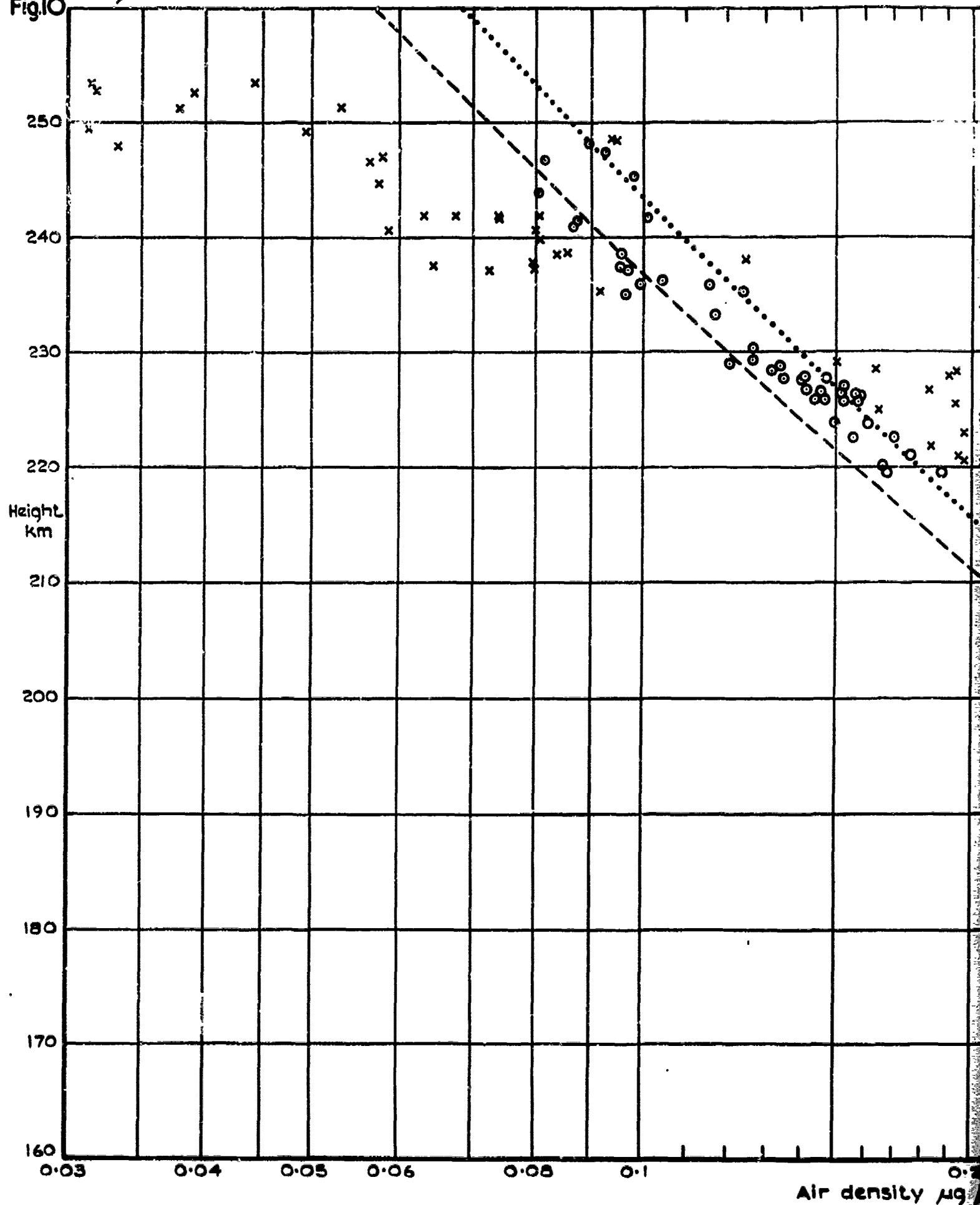


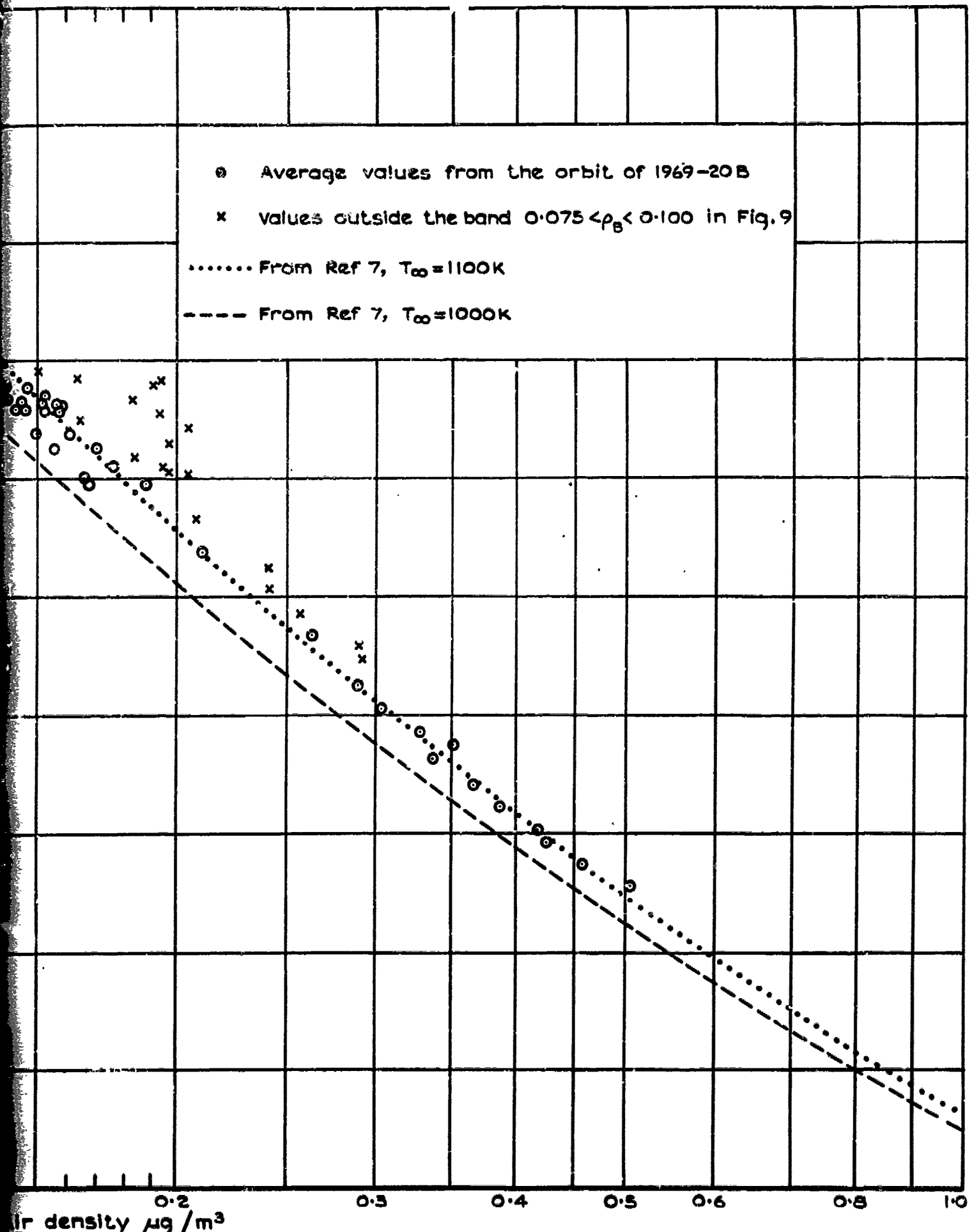
Fig.10 Variation of density with height from anal

21.1

21.2



75



T.R. 72071



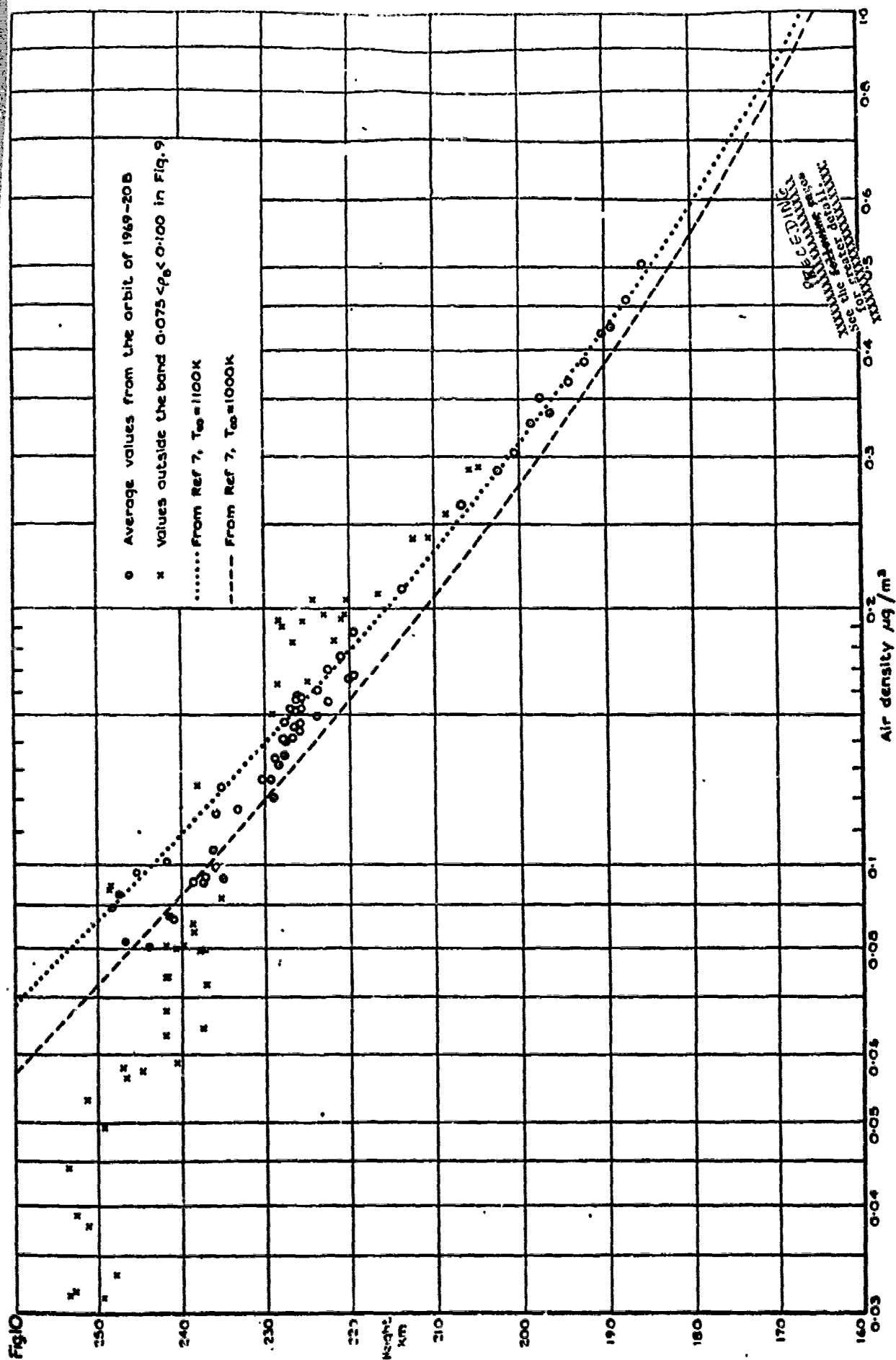


Fig. 10 Variation of density with height from analysis of the orbit of 1969-20B  $\lambda 1.3$

• 2000



Fig.11

- |                                 |                                      |
|---------------------------------|--------------------------------------|
| ▼ April/January density ratio   | — At 1070 km from 1964-63C (Ref 8)   |
| ■ April/July density ratio      | ---- At 185 km from 1967-31A (Ref 1) |
| ▲ October/July density ratio    | --- At 245-220 km from 1969-20B      |
| ● October/January density ratio |                                      |

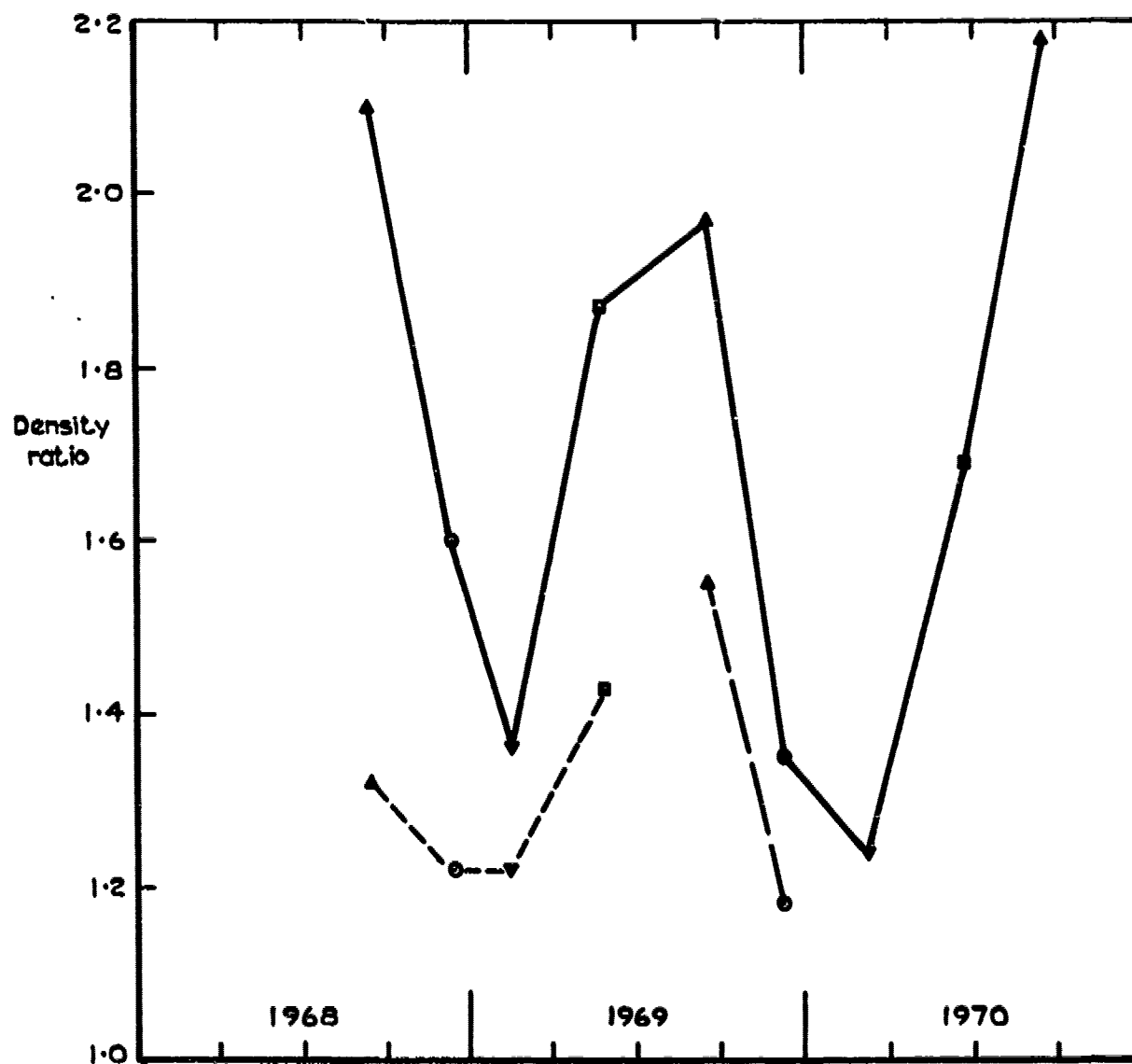


Fig.11 Magnitude of the semi-annual variation, 1968-70